Air Quality Control in Mine Refuge Chamber with Ventilation through Pressure Air Pipeline

Zujing zhang[a,b], Hongwei Wu[c], Kequan Wang[b], Rodney Day[c], Yanping Yuan[a*]

[a]School of Mechanical Engineering, Southwest Jiaotong University, Chengdu, 610031, China
[b]Chongqing Research Institute of China Coal Technology & Engineering Group, Chongqing, 400037, China
[c]School of Engineering and Computer Science, University of Hertfordshire, Hatfield, AL10 9AB, United Kingdom
[*]Corresponding author. Email: ypyuan@home.swjtu.edu.cn

Abstract: A combined experimental and numerical study was performed to improve the performance of the ventilation system in a mine refuge chamber (MRC). In the experiment, CO_2 cylinders and dispersion pipes were used to simulate the CO_2 release of 50 people, and 0.1 L/min per person of fresh air was provided by an air compressor. A new analytical model for a 50-person MRC was proposed and validated against the experimental data. Sensitivity analysis was carried out to investigate the effects of several control factors. The results indicated the following: (1) The ventilation system layout has a significant influence on the CO_2 concentration distribution in an MRC, while the uniformity of the CO_2 concentration distribution in the MRC may not be effective with increased number of air inlets. (2) Under a well-arranged ventilation system in the 50-person MRC, the average CO_2 concentration can be controlled at less than 0.5% with a ventilation rate of 0.1 m^3/min per person, and less than 0.2% with a ventilation rate of 0.3 m^3/min per person. (3) A quantitative correlation exists between the CO_2 concentration and ventilation volume rate, as well as the CO_2 release rate, for an MRC under a well-arranged ventilation system.

Keywords: Underground; Mine refuge chamber; Ventilation; CO_2 concentration; Air quality.

1 Introduction

Underground coal mining is a very dangerous operation owing to accidents involving gas explosion, water inrush, and roof collapse, among others (Tripathy and Ala, 2018). In China, it has been reported that over 90% of mine accidents with 10 or more casualties were mainly a result of explosion, water inrush, and fire, of which more than 60% were explosion accidents (Wang et al., 2014a; Zhu et al., 2019). Nearly 90% of the victims died of CO poisoning and asphyxia in coal mine explosion accidents (Vaught et al., 2000; National Research Council, 2013; Wang et al., 2014b) and 80% of the victims died indirectly from the flue gas in fire accidents (Charles and Inoka, 2012; Hansen and Haukur, 2013). Moreover, in China, 44% of coal mine explosion accidents had rescue times of more than two days (He et al., 2019). An effective method for solving the problem of personnel being harmed by fire and smoke is to establish life-saving facilities in the underground roadway (Zhang et al., 2012). A mine refuge chamber (MRC) is regarded as one such major life-saving facility that can provide a safe environment for miners in distress for no less than 96 h in coal mines (Bauer and Kohler, 2009; Margolis et al., 2011). The removal of the CO_2 accumulated in an MRC is one of the key requirements for breathable air (Mejías et al., 2014). However, this is a challenging issue owing the lack of electric power following an accident and the explosion-proof requirements of the electrical equipment in a coal mine.

It has been recognised that human metabolism is the main source of harmful gases in an MRC. The harmful gases produced by human metabolism are mainly CO_2, accompanied by trace harmful gases such as CO, H_2S, and NH_3. Among these, CO_2 has been proven to be a direct contaminant and used as an indicator of air quality for numerous years (Jia et al., 2018). Zhai et al. (2018) indicated that, for an adult man, the CO_2 metabolism rate is 199 mL/min when lying down, 228 to 287 mL/min when sitting down, and 237 to 300 mL/min when standing up.

Nomenclature

a	Constant in *Cst* expression	***Subscripts***	
c_0	Initial volume concentration	exp	Experimental data
C_1, C_2,	Turbulence model parameter	in	Air inlet
$C_{1\varepsilon}$, $C_{3\varepsilon}$	Turbulence model parameter	i, j	Elemental directions (i, j=1, 2 and 3 corresponding to the x, y, and z directions)
c	Volume concentration		
C_p	Thermal capacity of air, J/(kg·K)	num	Numerical data
D_s	Component diffusion coefficient	out	Air outflow
g	Gravitational acceleration, m^2/s	*sta*	*Stable*
G	Ventilation volume rate, m^3/s	***Greek symbols***	
G_b	Generation of turbulence kinetic energy due to buoyancy ($J/s\cdot m^3$)	σ_k, σ_ε	Turbulence model parameter
		Θ	Difference
G_k	Generation of turbulence kinetic energy due to the mean velocity gradients ($J/s\cdot m^3$)	ρ	Air density, kg/m^3
		λ	Air thermal conductivity, W/(m·K)
k	Turbulent kinetic energy (J/kg)	ε	Turbulent energy dissipation (J/kg·s)
N	Number of people	β	Coefficient of thermal expansion, 1/K
p	Pressure, Pa	μ	Dynamic viscosity, kg/m·s
S	Modulus of the mean rate-of-strain tensor	μ_τ	Turbulent eddy viscosity, (kg/m·s)
S_s	Component production rate	υ	Kinematic viscosity (m^2/s)
T	Temperature, °C	τ	Time, s
u	Air velocity, m/s	***Acronyms***	
v	CO_2 release rate per person, m^3/s	ATSI	Air temperature slow increase
V	Volume, m^3	MRC	Mine refuge chamber
x	Coordinate direction vector	PCA	Personnel concentrated area
		RSS	Relatively stable state

The CO_2 concentration has a certain influence on the indoor environmental comfort (Cheung et al., 2017). Li et al. (2018) stated that, when people are exposed to an environment with a CO_2 concentration of 12,000 ppm and relative humidity of 85%, significant headache symptoms can easily be observed. Zhang et al. (2016a) concluded that exposure to an environment with a CO_2 concentration of 5,000 ppm for 2.5 h did not increase the intensity of health symptoms of healthy college students when they performed simple or moderately difficult cognitive tests and certain tasks resembling office work. Liu et al. (2017) indicated that exposure to an environment with a CO_2 concentration of 3,000 ppm and a temperature of 35 °C did not cause any change in the measurable responses of people. However, new evidence suggests that CO_2 concentrations below the occupational level of 5,000 ppm may affect the ability to make decisions, although these levels have not been demonstrated to cause negative effects on health or comfort, or result in measurable physiological responses (Persily, 2015; Gall et al., 2016). Kajtar et al. (2012) concluded that exposure to 3,000 or 4,000 ppm CO_2 for several hours results in decreased cognitive performance via a proof of reading exercise. Du et al. (2018) recommended that the conditions for an MRC should be controlled with an O_2 volume fraction of approximately 18% to 22.7% and a CO_2

volume fraction of less than 1%.

An air curtain system was used to prevent harmful gases from pouring into the MRC and thereby to reduce the influence of harmful gas in the underground roadway on the MRC air quality (Zhang et al., 2016b; Wang et al., 2017). Three methods have been proposed to control the concentration of harmful gases in an MRC at an acceptable level: a hangable lithium hydroxide curtain, air purification devices, and ventilation. Jia et al. (2014) investigated the performance of three materials, namely $Ca(OH)_2$, LiOH, and NaOH, as CO_2 absorbents, and the results indicated that the reaction rates of these three materials with CO_2 gas from fast to slow were NaOH, LiOH, and $Ca(OH)_2$. Gao et al. (2015) investigated the application of KO_2 to supply oxygen and remove CO_2 gas. Their results demonstrated that, for a 15 g KO_2 solid plate formed by pressure extrusion at 10 kN, the average oxygen production rate is 11.88×10^{-3} L/min, while the average CO_2 absorption rate is 11.0×10^{-3} L/min. Gai et al. (2016) developed a purification device accompanied by a novel modified soda lime for an MRC. It was found that the optimal combination of soda lime with different mass fractions was 6% additives, 12% H_2O, and 6% NaOH, while the most effective working mode for the purification device was 25 W of fan power. Du et al. (2018) developed a novel modified soda lime with higher adsorption properties. Their results demonstrated that the adsorption capacity was increased by 36.2% and the adsorption rate was increased by 39.5% compared to normal soda lime. The modified soda lime was added to an air-purifying device, in which power was provided by explosion-proof axial flow fan air circulation (Du, 2017). Zhang et al. (2017) studied the layout of the air purification devices in a 50-person MRC. Their results indicated that two air-purifying devices can meet the air quality control requirements in the MRC, and the appropriate distribution of the two devices is one at each end of the MRC.

Ventilation is an effective measure of the oxygen supply and CO_2 removal in an MRC, for which a borehole from the surface directly to the MRC is the most advantageous and reliable option. For example, the 33 existing coal MRCs in the United States use ground boreholes to supply fresh air (Trackemas et al., 2015). The ventilation volume rate for MRCs should not be lower than 0.3 m^3/min per person, according to the *Policy on the construction and management of the coal mine underground emergency refuge system* in China (National Coal Mine Safety Administration, 2013). However, this is not realistic for certain coal mines, as the fresh air for the MRC is supplied by the existing mine air pressure system. According to the “Coal Mine Safety Regulations (2016)” of China, the acceptable minimum ventilation rate for a mine air pressure system is 0.1 m^3/min per person. Through theoretical calculations, Gao et al. (2012) determined that an air supply volume of 90 L/min per person can meet the indoor CO_2 concentration control requirements in an MRC. Shao et al. (2016) numerically investigated the variations in the CO_2 concentration in an MRC with one air inlet and one air outflow. It was found that the average CO_2 concentration in the MRC was maintained at 1% when the CO_2 release rate was 0.41 L/min per person and the ventilation rate was 42 L/min per person. You et al. (2012) and Jin (2013) conducted an experiment to control the air quality in an 80-person MRC by means of ventilation. The MRC was located underground of the Changcun Coal Mine in Shanxi province, China, as illustrated in Fig. 1. Their results demonstrated that, when the ventilation rate was 100 L/min per person, the CO_2 and O_2 concentrations in the MRC could be maintained at approximately 0.3% to 0.34% and 19.6% to 19.8%, respectively. He (2017) conducted an experiment to control the air quality in a 50-person MRC using ventilation. The results indicated that the minimum ventilation rate for meeting the air quality control requirements was 84 L/min when the CO_2 release rate was 0.5 L/min per person.

In general, previous research on air quality control in an MRC mainly focused on the development of air purification devices, CO_2 adsorption, and the ventilation volume rate that can meet the air quality control requirements in an MRC. It is well known that the ventilation system layout plays an important role in the air quality distribution in an MRC, but few, if any, studies have focused on this aspect. Thus, it is imperative to improve the ventilation system for air quality in the MRC. In this work, a combined experimental and numerical study was performed to investigate the effects of the air inlet and air outflow layout, the ventilation volume rate, and the CO_2 release rate by refugees on the CO_2 concentration distribution in an MRC under ventilation.

Fig. 1 Experimental scene of air quality control for 80-person MRC by ventilation. [36]

2 Experimental setup

2.1 Experimental environment and principles

The experiment was conducted in a comprehensive MRC laboratory with inner dimensions of 20 m in length, 4 m in width, and 3 m in height. A screw air compressor (DFB-100A) with a volume flow rate of 11.3 m^3/min was used to supply fresh air to the MRC, whereby the fresh air entered the MRC through buried ventilating pipes. The ventilation volume rate was controlled by a total valve. There were three muffler air inlets on each side of the long channel. The air inlets were arranged 1.8 m above the ground, and the distance between two adjacent air inlets was 3.5 m. A one-way automatic exhaust valve with a diameter of 110 mm was installed at each end wall of the MRC as the air outflow. The exhaust valve opened automatically to vent the contaminated air when the relative pressure in the MRC reached 180 Pa. Both air outlets were located 2.4 m above the ground. Figure 2 illustrates the experimental environment, equipment, and instruments.

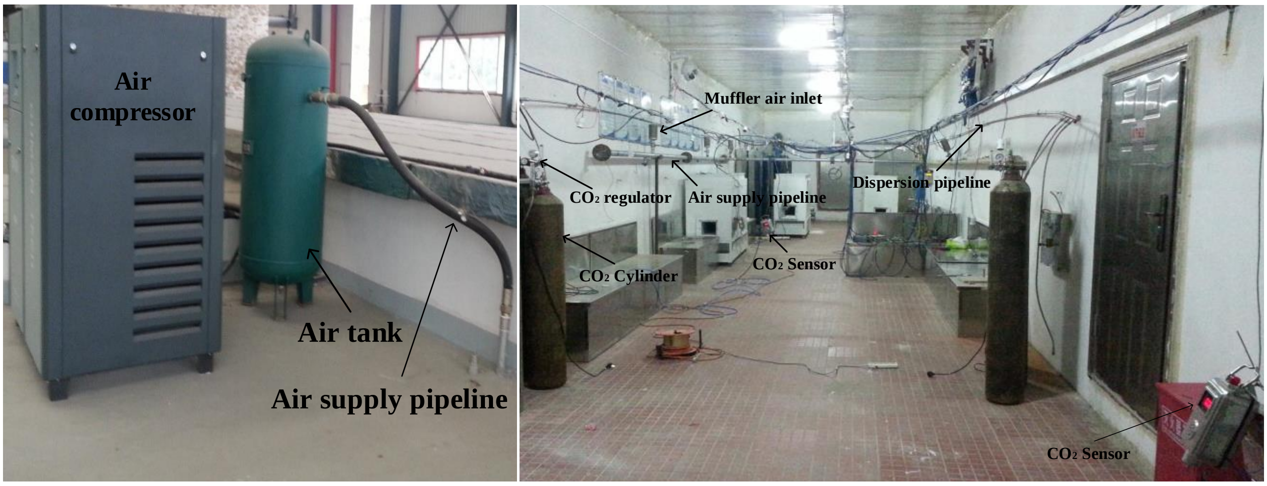

Fig. 2 Experimental environment and equipment.

According to temporary provisions, the CO_2 concentration (in volume) in an MRC cannot be less than 1%, and the capacity for CO_2 removal cannot be less than 0.5 L/min per person. To save on time and costs, the initial CO_2 concentration in an MRC is approximately 1%. The "Coal Mine Safety Regulations (2016)" in China stipulates that the average air supply of the pressurised air self-rescue device should be no less than 0.1 m^3/min per person. Therefore, in the experiment, the ventilation volume rate was set to 300 m^3/h (0.1 L/min per person). To ensure that the CO_2 release rate was maintained at a constant value of 0.5 L/min per person, high-pressure CO_2 cylinders and dispersion gas supply pipes were used to replace the CO_2 release rate of people. The CO_2 gas was released from the high-pressure CO_2 cylinders and then entered the MRC through diffusion air-supply pipes that were installed on both sides of the room. The diffusion gas supply pipeline was a stainless steel pipe with a 15 mm diameter and 10 m length. The diameter of the gas supply hole was 1.5 mm, and the distance between two adjacent holes was 100 mm. The CO_2 release rate entering the MRC was 25 L/min to simulate the CO_2 released by 50 people.

It should be noted that the CO_2 release channel in this experiment differed from that in practical conditions for an MRC, which could result in several differences in the CO_2 concentrations at the various measuring points. However, under the same operating conditions of the CO_2 release rate, ventilation rate, and layout of the air inlets and outlets, the error of the indoor average CO_2 concentration produced by simulating human exhalation of CO_2 through a CO_2 cylinder will be relatively small. In this study, a comparative experiment was conducted to reduce the calculation error of the average CO_2 concentration caused by the different measuring points. Two fans were used to stir the indoor air to make the CO_2 concentration distribution more uniform, while the other experimental parameters were maintained the same.

2.2 Measurement and data acquisition

There were seven measurement points for measuring the CO_2 concentration in the MRC. The distribution of the measurement points is illustrated in Fig. 3.

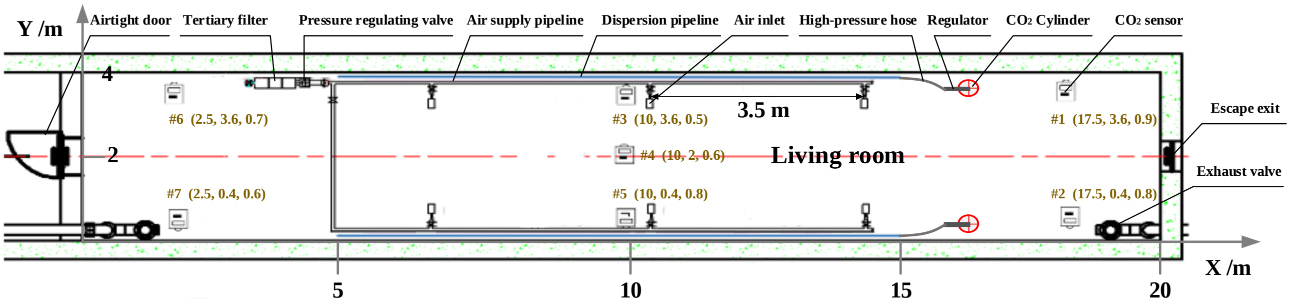

Fig. 3 Layout of air supply inlets and measurement points in living room.

The CO_2 concentration in the living room was monitored by infrared CO_2 sensors (GRG5H, Chongqing Research Institute of China Coal Technology and Engineering Group Co., Ltd.) in real time. The monitoring data were collected and saved automatically by the monitoring system platform. The ventilation volume rate for the living room was measured using a vortex flowmeter (SLDLUGB-DN50, Nanjing Senlod Measurement and Control Equipment Co., Ltd.) that was installed in the air-supply pipeline. The CO_2 release rate was measured by an electrically heated CO_2 decompression valve with a float flowmeter (YQT-731LR, Shanghai Regulator Co., Ltd.), which was linked to the high-pressure CO_2 cylinders. Figure 4 illustrates the interface between the measuring instruments and data acquisition system platform.

(a) Vortex flowmeter (b) CO_2 decompression valve (c) CO_2 sensor (d) Data acquisition platform

Fig. 4 Testing instruments and data acquisition system.

2.3 Experimental procedure

(1) The sensors were checked to ensure that they were working correctly and the data could be uploaded to the monitoring system platform.

(2) Operators entered the living room and closed the airtight door.

(3) The control valve of the CO_2 cylinder was opened and the flow rate of the CO_2 decompression valve was regulated at the maximum, so that the CO_2 concentration in the chamber increased to approximately 1%.

(4) The electric fans were turned on to stir the gas in the MRC until the CO_2 concentration approached 1%. (In the comparison experiment, the two fans were constantly running.)

(5) The CO_2 relief valves were adjusted to ensure that the CO_2 release rates on the two sides were 12 and 13 L/min, respectively.

(6) The air compressor was opened and the valve was adjusted to ensure that the ventilation volume rate for the MRC was 300 m^3/h.

(7) The test was terminated once the CO_2 volume concentration was relatively stable in the living room.

3. Computational details

To optimise the layout of the air inlets and outlets of the ventilation system in the MRC, and to compute the optimum ventilation volume rate for an MRC, numerical analysis was also performed using ANSYS Fluent, which was consistent with the above experiment.

3.1 Computational model

For comparison with the above experimental results, a computational model of a 50-person MRC with an internal size of 20 m in length, 3 m in height, and 4 m in width was established. Considering the influence of the human body on the room space, a human model was incorporated into the computational model. The surface area and volume of the human model were 2 m^2 and 0.067 m^3, respectively. A square with an area of 0.08 m^2 was included on the head as the breathing gas outlet. A total of 50 people were divided into four rows in the room. Among these, there were 13 people in each row near the two sides 0.3 m from the adjacent wall, and 12 people in each of the two middle rows, with a 0.4 m gap between two people's backs. The distance between two adjacent people in the same row was 1 m. The human bodies were placed 0.35 m above the ground to obtain high-quality boundary layer grids. To analyse the effects of the layout of both the air inlets and outflows on the CO_2 concentration distribution in the MRC, 20 air inlets with a diameter of 0.075 m, four air outflows with a diameter of 0.225 m, and one air outflow with a diameter of 0.32 m were pre-positioned in the computational model. A total of 10 air inlets were located at the top of the MRC in two rows, with a row distance of 2 m, while the other 10 air inlets were located at either side of the MRC, at a distance of 1.8 m above the ground. The distance between two adjacent air inlets in the same row was 3.5 m. Two air outflows of the same area were located at the upper and lower parts of each wall at both ends of the MRC. The lower and upper air outflows were 0.3 and 2.7 m from the ground, respectively. The outlet with a diameter of 0.32 m was located at the upper part of the left end wall, 2.5 m from the ground. The geometric model of the 50-person MRC is illustrated in Fig. 5.

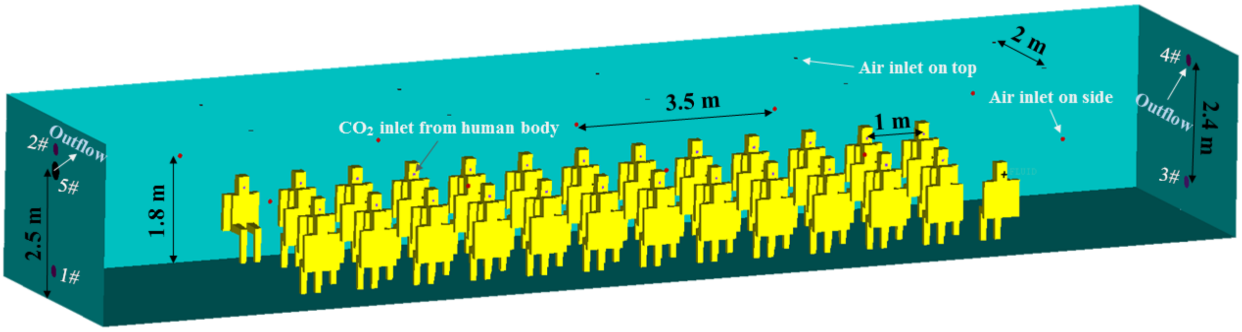

Fig. 5 Geometric model of 50-person MRC.

The grids of the computational geometry were generated by ANSYS ICEM. Unstructured mesh was used owing to the complexity of the model structure. A grid independence study was performed to ensure that the numerical results were independent of the grid. Five grid models with different numbers of cells, namely 1.12×10^6, 1.68×10^6, 2.31×10^6, 3.34×10^6, and 4.51×10^6, were analysed under the same conditions. Figure 6 presents a comparison of the CO_2 concentration in the MRC at 1 and 2 h using the five different grids. It can be observed from Fig. 6 that, when the number of cells in the numerical model reached 2.31×10^6, the numerical results were not strongly affected by the number of grids. Therefore, considering the computational accuracy and resources, the grid model with 2.31×10^6 cells was used for the following numerical analysis.

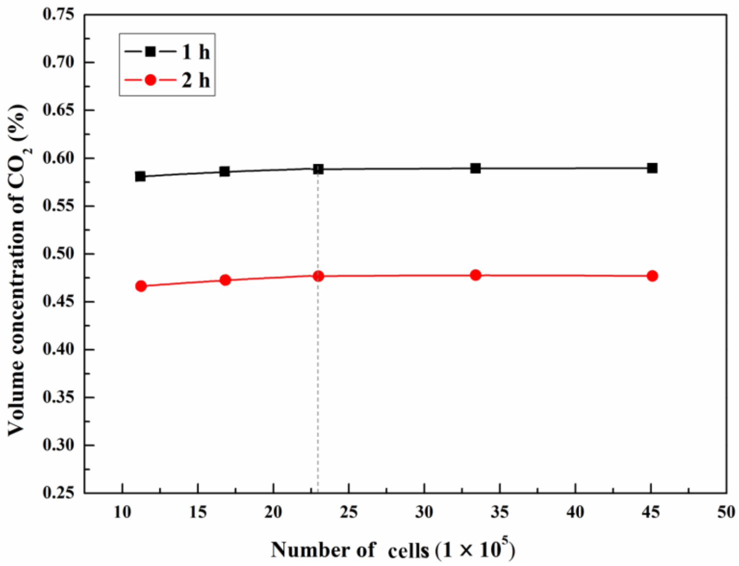

Fig. 6 Comparison of CO_2 concentrations in MRC at 1 and 2 h using five different grids.

3.2 Boundary conditions

In this work, trace gases such as CO, NH_3, SO_2, and NH_3 existing in the air environment and produced by human metabolism were neglected. The CO_2 gas was regarded as an indicator of the MRC air quality.

The human-exhaled gases were composed of O_2, N_2, CO_2, and water vapour, the volume fractions of which were 16%, 78%, 4%, and 2%, respectively. The area for the human-exhaled gases was the inlet of the exhaled gas into the MRC. The velocity of the exhaled gas inlet was calculated according to the area of the exhaled gas inlets and CO_2 release rate. The velocity was 0.13 m/s when the CO_2 release rate was 0.5 L/min per person. The temperature of the exhaled gas was 35 °C, and the surface of the human body was defined as a constant temperature wall of 32 °C.

The volume fractions of the O_2, N_2, CO_2, and water vapour in the fresh air for the air inlets were 21%, 78%, 0.03%, and 0.97%, respectively. In the model, six air inlets simultaneously delivered fresh air to the MRC at the same velocity. The velocity of the air inlets was calculated according to the area of the air inlets and ventilation volume rate of the MRC. The velocity was 3.204 m/s when the ventilation volume rate was 300 m^3/h. The temperature of the air inlets was 32 °C.

The MRC exhaust vent was set as the air outflow. The number of air outflows was determined in terms of the working conditions. The walls of the MRC and other surfaces were set to a constant heat flux boundary with a heat flux rate of 0 W/m^2.

In the initial air environment, regardless of the water vapour, the volume fractions of the O_2, N_2, and CO_2 were 20.5%, 78%, and 1.05%, respectively. The initial temperature was 25 °C.

3.3 Turbulence model

In this study, five operating conditions with different ventilation rates, namely 100, 150, 200, 250, and 300 L/min per person, were considered. The velocity of the air inlets ranged from 3.2 to 9.6 m/s. As the Reynolds number at the air inlet could be calculated as 9,091 to 29,032, the airflow in the MRC was turbulent.

The realizable k–ε turbulence model was used because it exhibits strong performance with indoor airflows, temperature, and pressure in closed structures (Sørensen and Nielsen, 2003;

Bacharoudis et al., 2007; Piña-Ortiz et al., 2014; Wu et al., 2015). Enhanced wall treatment and a full buoyancy effect were considered in the turbulence model. The pressure gradient and thermal effect were neglected in the boundary function. Species transport was used for the component analysis. The gaseous components, including O_2, N_2, CO_2, and water vapour, were loaded into the material item from the fluid material database.

The governing equations of the mass, momentum, and energy were given as follows (Wu et al., 2015):

$$\frac{\partial \rho}{\partial \tau}+\frac{\partial(\rho u_i)}{\partial x_i}=0 \tag{1}$$

$$\frac{\partial u_i}{\partial \tau}+\frac{\partial(u_i u_j)}{\partial x_j}=-\frac{1}{\rho}\frac{\partial P}{\partial x_i}+\frac{1}{\rho}\frac{\partial}{\partial x_j}\left[\mu\left(\frac{\partial u_i}{\partial x_j}+\frac{\partial u_j}{\partial x_i}\right)-\rho\overline{u_i' u_j'}\right]-g_i\beta\left(T-T_0\right) \tag{2}$$

$$\frac{\partial T}{\partial \tau}+\frac{\partial(u_j T)}{\partial x_j}=\frac{1}{\rho}\frac{\partial}{\partial x_j}\left(\frac{\lambda}{c_p}\frac{\partial T}{\partial x_j}\right) \tag{3}$$

The heat source was not considered in the energy equation, as the human surface was treated as a constant temperature wall. The viscous dissipation could be ignored because almost no mechanical energy was converted into heat.

The mass conservation equation of the component was (Zhang et al., 2012):

$$\frac{\partial\left(\rho c\right)}{\partial \tau}+\frac{\partial(\rho u_j c)}{\partial x_j}=\frac{\partial}{\partial x_j}\left(D_s\frac{\partial(\rho c)}{\partial x_j}\right)+S \tag{4}$$

Two transport equations were formulated for the realizable *k*–*ε* model, as follows (Boulet et al., 2010):

$$\frac{\partial k}{\partial \tau}+\frac{\partial(k u_j)}{\partial x_j}=\frac{1}{\rho}\frac{\partial}{\partial x_j}\left[\left(\mu+\frac{\mu_\tau}{\sigma_k}\right)\frac{\partial k}{\partial x_j}\right]+\frac{G_k+G_b}{\rho}-\varepsilon \tag{5}$$

$$\frac{\partial \varepsilon}{\partial \tau}+\frac{\partial(\varepsilon u_j)}{\partial x_j}=\frac{1}{\rho}\frac{\partial}{\partial x_j}\left[\left(\mu+\frac{\mu_\tau}{\sigma_\varepsilon}\right)\frac{\partial \varepsilon}{\partial x_j}\right]+C_1 S\varepsilon+C_2\frac{\varepsilon^2}{k+\sqrt{\upsilon\varepsilon}}-C_{1\varepsilon}\frac{\varepsilon}{k}C_{3\varepsilon}G_b \tag{6}$$

3.4 Calculation parameters

In this work, the Boussinesq assumption was used for the air operating density, taking the gravity into account. The pressure-implicit with splitting of operators algorithm was applied. The under-relaxation factors were 0.8 for the pressure, 0.2 for the momentum, and default values for the other terms. The turbulence parameters of the air inlets, namely the turbulence intensity, turbulence length scale, turbulence kinetic energy, and turbulence dissipation energy, were set as default values. The pressure, power, turbulent kinetic energy, energy, time, and components were discretised by the second-order upwind method. The convergence absolute criterion was 10^{-6} for energy and 10^{-3} for the other items. The calculation was convergent when the time step ranged from approximately 0 to 5 s, and it was demonstrated that the numerical result was independent of the time step. In this work, the time step was 5 s.

4 Results and discussion

4.1 Variations in CO_2 concentration

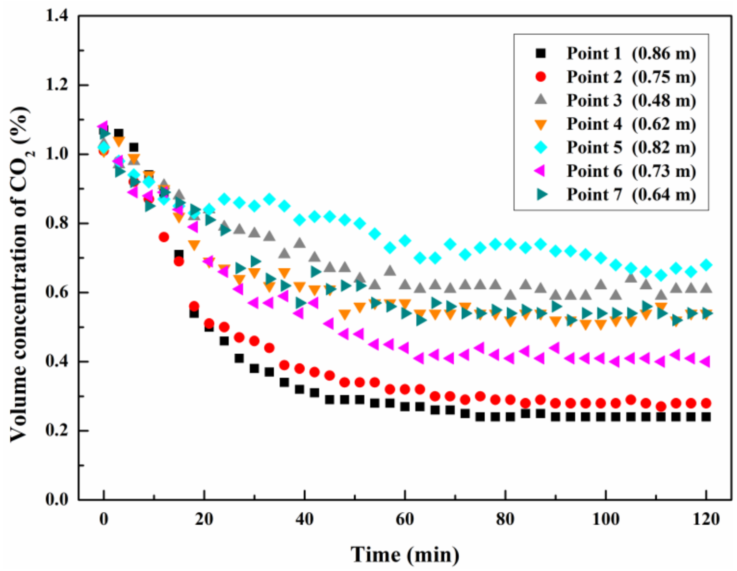

Fig. 7 Variations in CO_2 concentration with time with ventilation volume rate of 300 m³/h.

Figure 7 plots the variations in the CO_2 concentration at different measuring points when the ventilation volume rate was maintained at 300 m^3/h. It can be observed from Fig. 7 that, in the MRC with an initial CO_2 concentration of 1.1%, the CO_2 concentration exhibited a decreasing trend and gradually tended towards a stable value when the ventilation volume rate was 300 m³/h. This indicates that, when the CO_2 release rate was 0.5 L/min and the ventilation volume rate was 0.1 m^3/min per person, the average CO_2 concentration in the MRC could be controlled below 1%. At the beginning of the ventilation, the CO_2 concentration decreased significantly, and it took approximately 1 h to reach a relatively stable state (RSS). It can be observed that, once the CO_2 concentration in the MRC reached the RSS, the CO_2 concentration value at each measurement point differed significantly, ranging from 0.25% to 0.75%, and the concentration difference between the highest and lowest points was approximately 0.5%. This implies that the uniformity of the CO_2 concentration distribution in the MRC was poor.

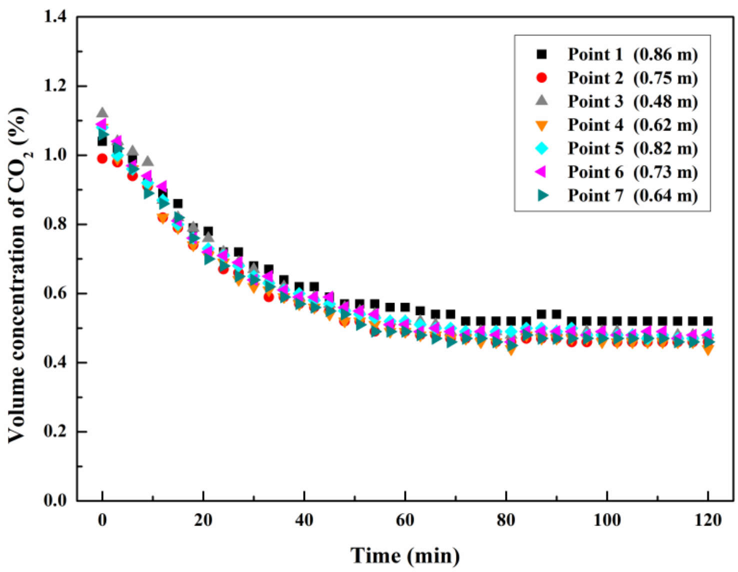

Fig. 8 Variations in CO_2 concentration with time under combined action of air supply and fan stirring.

Figure 8 illustrates the variations in the CO_2 concentration at the measuring points when the ventilation volume rate for the MRC was 300 m^3/h under the action of fan stirring. It can be observed from Fig. 8 that, when the ventilation volume rate was 300 m^3/h and the fans were working to stir the indoor air, the CO_2 concentration in the MRC also exhibited an obvious decreasing trend within 1 h until reaching the RSS. The CO_2 concentration at the RSS stage ranged from 0.45% to 0.52%, and the concentration difference between the measuring points was less than 0.1%. It should be noted that the disturbance of the fans caused the CO_2 concentration to be evenly mixed in the MRC.

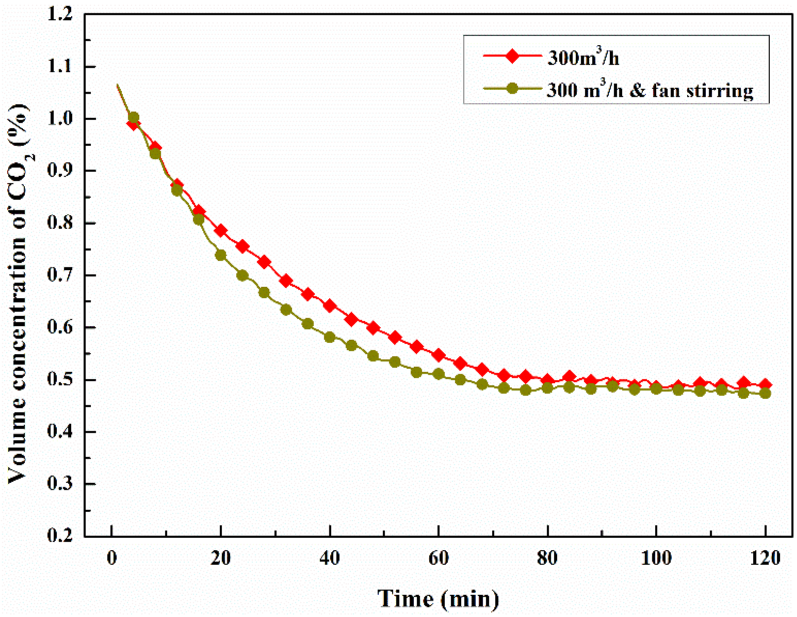

Fig. 9 Comparison of average CO_2 concentrations for conditions with and without fan stirring.

Figure 9 compares the average CO_2 concentrations of these measuring points with and without fan disturbance. It can be observed from Fig. 9 that, before the CO_2 concentration in the MRC tended to become stable, the average CO_2 concentrations of the measuring points with stirring were lower than those without, and the maximum difference between the two was approximately 0.06%. However, the variation trend of the average CO_2 concentration was not significantly affected by the fan stirring. The time of the CO_2 concentration entering the RSS was very close for these two cases, at approximately 70 to 80 min. During the RSS stage, the average CO_2 concentrations of these two cases were almost the same, with a concentration difference of less than 0.02%. Thus, it can be inferred that, even when the indoor airflow rate differs, the average CO_2 concentration in the MRC when reaching the steady state will be almost the same under the same layout of air inlets and air outlets, total CO_2 release rate, and ventilation volume rate.

The experimental results demonstrated that, when the CO_2 release rate was 0.5 L/min and the ventilation volume rate was 0.1 m^3/min per person, the CO_2 concentration in the MRC could be effectively controlled below 0.8%, and the average CO_2 concentration was approximately 0.5%. However, the CO_2 concentration distribution in an MRC is not uniform under ventilation, and the air quality may be affected by poor ventilation systems owing to a higher CO_2 concentration in a local area. Thus, it is very important to improve the ventilation system layout to achieve acceptable air quality in the MRC.

4.2 Validation of numerical model

To verify the applicability of the numerical model, the numerical results were compared with the results of the above experiment without fan stirring. It should be noted that the distribution of the human CO_2 release outlets in the numerical model differed from that in the experiment, but the total CO_2 release rate was the same. Moreover, both the installation positions of the air inlets and the ventilation volume rate were the same in the numerical model and experiment, although there was a slight difference in the air inlet shape.

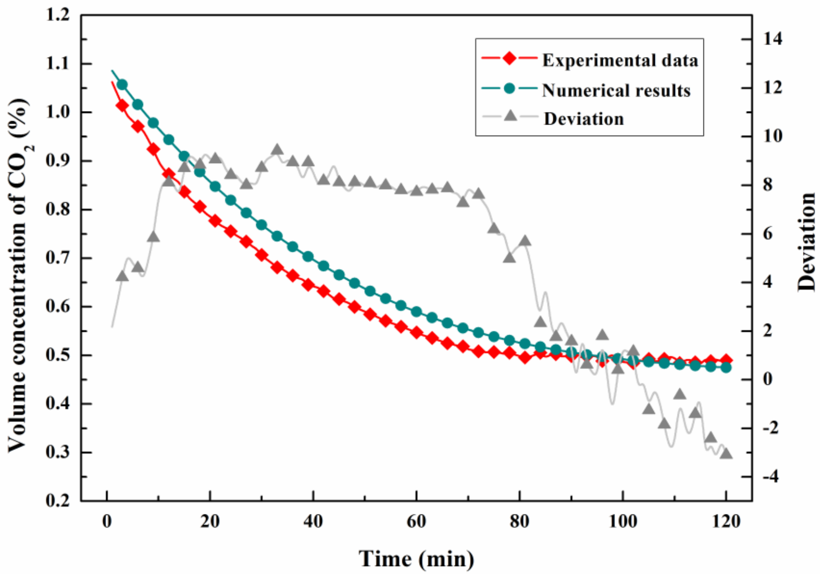

Fig. 10 Comparison of numerical results and experimental data.

Figure 10 compares the average CO_2 concentrations of the measuring points varying with time in the MRC for the numerical analysis and experiment. The deviation between the numerical results and experimental data was calculated based on the average CO_2 concentration of the experiment, namely $\Theta = (C_{\mathrm{Num}}-C_{\mathrm{Exp}})/C_{\mathrm{Exp}}$. It can be observed from Fig. 10 that the predicted CO_2 concentration agreed well with the experimental data. The CO_2 concentration decreased rapidly from approximately 1.1% to 0.5% within approximately 70 to 80 min until it entered the RSS. From 0 to 1 h, the numerical results were slightly higher than the experimental data, the maximum difference in the CO_2 concentration was less than 0.7%, and the deviation was less than 10%. After reaching the stable state, the difference between the values decreased to 0.2% and the deviation was less than 4%, indicating that the numerical model is effective.

4.3 Sensitivity analysis

In practice, the effect of the air quality control in an MRC is influenced by several control parameters, such as the CO_2 release rate of people, ventilation rate, ventilation system layout, and personnel distribution. Among these, the personnel distribution exhibits a certain randomness. In terms of the overall space arrangement in an MRC, the space at both ends of the MRC is generally occupied by some equipment and lockers for storing household or escape items, and people are usually arranged in several rows in the remaining space, with a certain distance for them to walk. The personnel distribution implemented in the numerical 50-person MRC is a very common distribution pattern, which makes full use of the indoor space, and is also convenient for people to walk and talk to each other. Therefore, in this study, the influence of the personnel distribution on the air quality control was not considered.

4.3.1 Layout of air inlets

A series of numerical analyses with different air inlet layouts were performed to investigate the effect of the layout of the air inlets on the CO_2 concentration distribution in the MRC. Under these conditions, an outflow was located at the top of each end, the ventilation volume rate was 300 m^3/h, and the CO_2 release rate was 0.5 L/min per person.

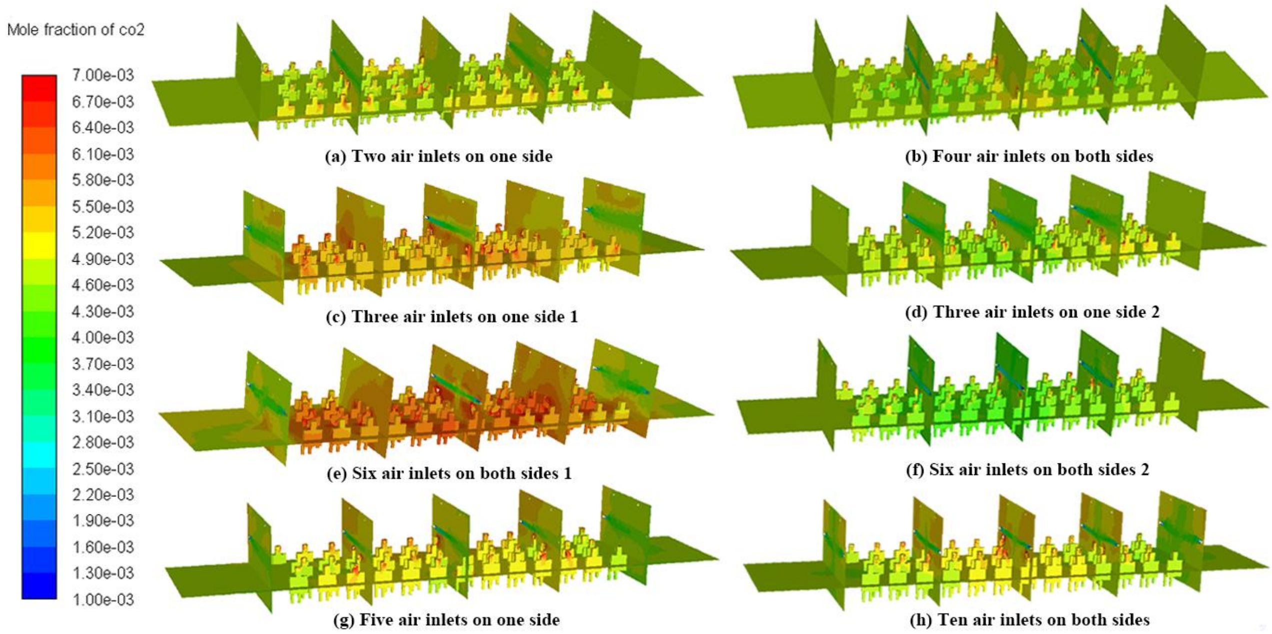

Fig. 11 Distribution of CO_2 concentration under different air inlet layouts at both sides.

Figure 11 illustrates the CO_2 concentration distribution when the ventilation volume rate was 300 m^3/h under different air inlet layouts at both sides of the MRC. It can be observed from Fig. 11 that, when the ventilation volume rate was 300 m^3/h, the CO_2 concentration ranged from 0.3% to 0.7%. Therefore, it can be concluded that a ventilation volume rate of 0.1 m^3/min per person can meet the requirements of controlling the CO_2 concentration in an MRC within 1%. However, the layout of the air inlets has an important influence on the CO_2 concentration distribution in the MRC.

According to Figs. 11(a), (c), (d), and (g), when the air inlets were located at one side of the tunnel, the CO_2 concentration distribution in Fig. 11(d) with three air inlets located in the personnel-concentrated area (PCA) was superior to that with the two air inlets (a). Moreover, when the number of air inlets increased to five and two of the inlets were located in the no-person area (g), the CO_2 concentration increased and the uniformity of the CO_2 concentration distribution in the MRC decreased obviously. It can be observed from Fig. 11(g) that the CO_2 concentration in the PCA was higher than that in the no-person area at both ends. Figures 11(c) and (d) clearly indicate that, for the cases with the same number of air inlets, the air inlets located in the PCA were obviously more conducive to air quality control than those distributed near both ends. Similarly, it can be observed from Figs. 11 (b) and (f) that, when the air inlets were arranged on both sides of the tunnel, the CO_2 concentration distribution under the condition of three air inlets located on each side of the PCA (f) was obviously superior to that of two air inlets located on each side (b). Comparing Fig. 11 (f) with (e) and (h), it can be observed that distributing or adding air inlets near both ends in the no-person area was not conducive to air quality control in the MRC. The reason is that the CO_2 concentration at both ends was relatively low when the air inlets were added into the no-person area, while the CO_2 concentration of the polluted air removed from the outflows was relatively low, which reduced the efficiency of fresh air replacing the CO_2 contaminated gases. Therefore, when air outflows are located at both ends and air inlets are arranged on both sides in an MRC, the air inlets should be located in the PCA.

Moreover, it can be observed from Figs. 11(d) and (f) that, in these two cases with three air inlets located on only one side of the PCA (d) and on each side of the PCA (f), the difference in the CO_2 concentration distribution was relatively small, ranging from 0.3% to 0.5%. However, when three air inlets were located on each side of the PCA, the CO_2 concentration in the PCA was obviously better distributed than that with only three air inlets located on one side. Therefore, when air outflows are located at both ends, air inlets evenly distributed on both sides of the PCA will be more conducive to the removal of harmful gases in the MRC.

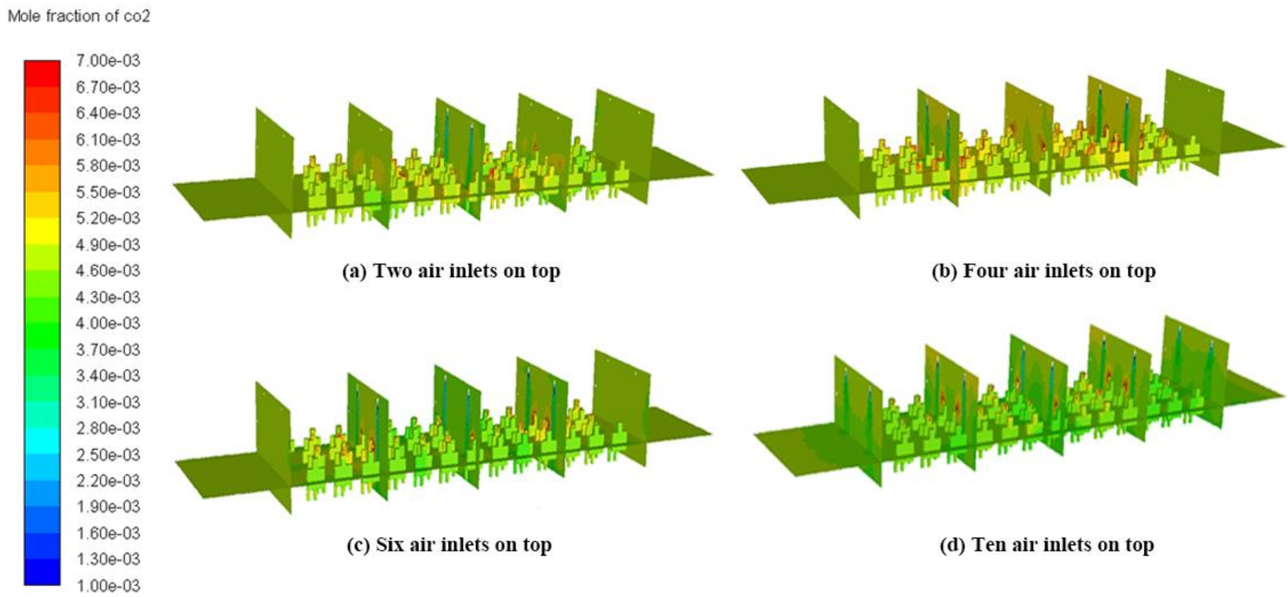

Fig. 12 Distribution of CO_2 concentrations under different air inlet layouts at top.

Figure 12 illustrates the CO_2 concentration distribution under different layouts of the air inlets located at the top of the MRC. It can be observed from Fig. 12 that, when the air inlets were located at the top of the MRC and the ventilation volume rate was 0.3 m^3/h, the CO_2 concentration in the MRC ranged from 0.3% to 0.6% under the four different air inlet layouts. It can be concluded that the CO_2 concentration distribution in the MRC was relatively uniform when only two air inlets were located at the top of the middle of the MRC, as indicated in Fig. 12(a). However, the CO_2 concentration uniformity decreased when four air inlets were located at the top, as illustrated in Fig. 12(b). It is obvious that the CO_2 concentration in the PCA was higher than that in the no-person area. When there were six air inlets located at the top of the PCA, as illustrated in Fig. 12(c), the CO_2 concentration in the PCA was lower than that in the no-person area, which is more conducive to controlling the harmful gas concentration in the MRC for refugees. Moreover, it can be concluded that the CO_2 concentration in the MRC was generally well distributed when the number of air inlets located at the top increased to 10, as indicated in Fig. 12(d).

Comparing Figs. 10 and 11, it can be determined that, when the fresh air flowed into the MRC from the top air inlets, the CO_2 concentration in the lower space of the MRC was lower than that in the higher space, which is conducive to controlling the air quality in the breathing area. However, there was no significant difference in the CO_2 concentration distribution between the cases with six air inlets located at both sides and six air inlets located at the top in the PCA.

4.3.2 Layout of air outflows

A series of numerical analyses with different air outflow layouts were performed to investigate the effect of the air outflow layout on the CO_2 concentration distribution in the MRC. In the simulation, the ventilation volume rate was 300 m^3/h and the CO_2 release rate was 0.5 L/min per person.

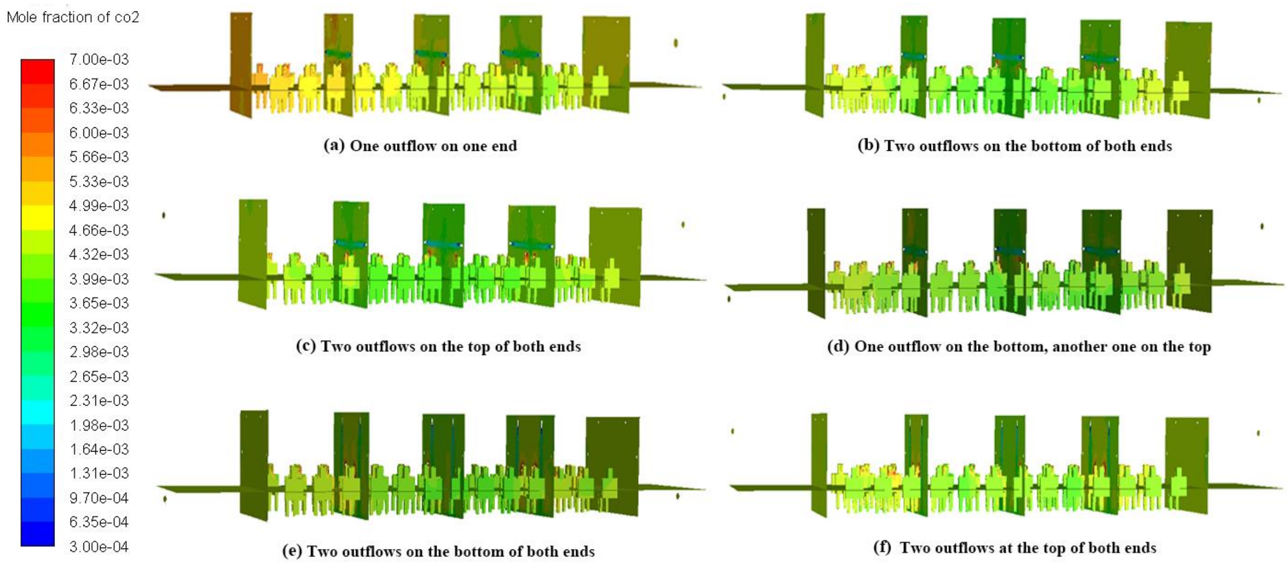

Fig. 13 Distribution of CO_2 concentration under different air outflow layouts.

Figure 13 illustrates the distribution of the CO_2 concentration in the MRC under different air outflow layouts. It can be observed from Fig. 13(a) that the uniformity of the CO_2 concentration in the MRC was poor when only one outflow was installed at one end. Moreover, the CO_2 concentration in the area near the end without outflow was higher than that in the area near the end with outflow. Furthermore, Figs. 13(b), (c), and (d) indicate that, under the same air supply conditions, when one air outflow was located at each end, there was no significant change in the CO_2 concentration distribution in the MRC, regardless of whether both air outflows were located at the upper part or lower part, or one was located at the upper part and the other at the lower part, respectively. Comparing Figs. 13(e) and (f), it can be concluded that, when six air inlets were distributed in two rows at the top of the MRC, the CO_2 concentration of the air outflows located at the top of each end was slightly lower than that of the air outflows located at the bottom of each end. This could be owing to the low CO_2 concentration in the lower space and high CO_2 concentration in the upper space when the air inlets were arranged at the top.

According to the results, it is necessary to arrange one outflow at each end of the wall on both ends of the MRC. The location of the outflow at the top or bottom of the wall has negligible effect on the CO_2 concentration distribution in the MRC.

4.3.3 Ventilation volume rate

To investigate the effect of the enhanced ventilation volume rate on improving the air quality in the MRC, five different ventilation volume rates, namely 0.1, 0.15, 0.2, 0.25, and 0.3 m^3/min per person, were analysed, with the other parameters remained the same. That is, three air inlets were located at each side and one outflow was located at the top of each end, and the CO_2 release rate was 0.5 L/min per person.

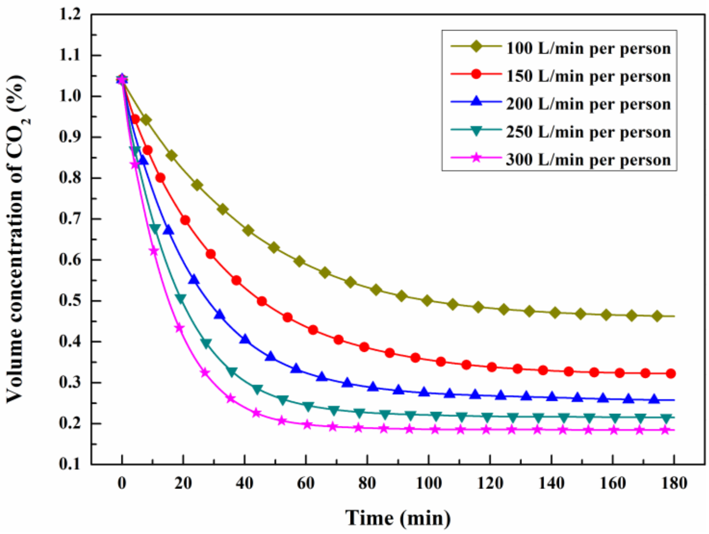

Fig. 14 Variations in CO_2 concentration with time under different ventilation volume rates.

Figure 14 plots the curves of the average CO_2 concentration in the MRC varying with time under different ventilation volume rates. It can be observed that, when the ventilation volume rate for the MRC was greater than or equal to 0.1 m^3/min per person, the average CO_2 concentration decreased with time until it tended towards a relatively stable value of less than 0.5%. With the increase in the ventilation volume rate, both the time to reach relative stability and the stable CO_2 concentration decreased. The time to reach the RSS was approximately 2 h when the ventilation volume rate was 0.1 m^3/min per person, and less than 1 h when the ventilation volume rate reached 0.3 m^3/min per person. The stable CO_2 concentrations for the five different ventilation rates of 0.1, 0.15, 0.2, 0.25, and 0.3 m^3/min per person were 0.483%, 0.32%, 0.257%, 0.215%, and 0.185%, respectively.

4.3.4 CO_2 release rate

To investigate the effect of the CO_2 release rate of human metabolism on the air quality control in the MRC, five different CO_2 release rates, namely 0.3, 0.35, 0.4, 0.45, and 0.5 L/min per person, were analysed, while the other parameters were maintained the same. That is, three air inlets were located at each side and one outflow was located at the top of each end, and the ventilation volume rate was 0.1 m^3/min per person.

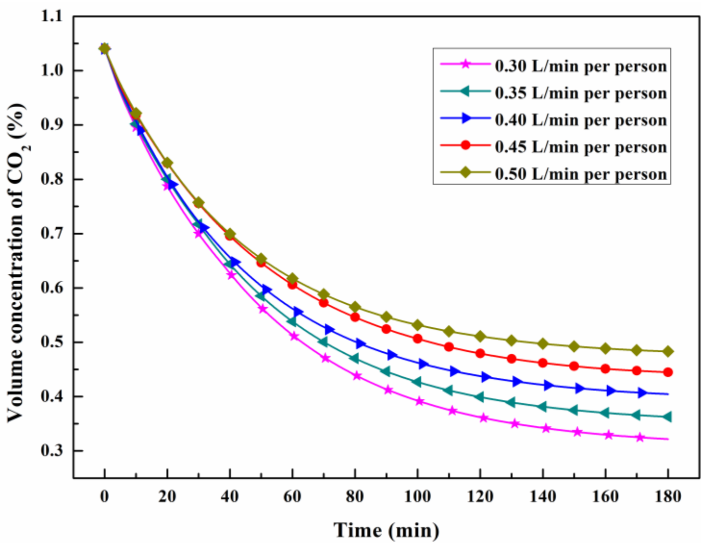

Fig. 15 Variations in CO_2 concentration with time under different CO_2 release rates.

Figure 15 plots the curves of the average CO_2 concentration in the MRC varying with time under different CO_2 release rates. It can be observed that, with the increase in the CO_2 release rate, the time to reach the steady state decreased but the stable CO_2 concentration increased. The time to reach the steady state was approximately 3 h when the CO_2 release rate was 0.3 L/min per person and approximately 2 h when the CO_2 release rate reached 0.5 L/min per person. The stable CO_2 concentrations for the five different CO_2 release rates of 0.3, 0.35, 0.4, 0.45, and 0.5 L/min per person were 0.322%, 0.363%, 0.404%, 0.445%, and 0.483%, respectively.

4.4 Discussion

4.4.1 Prediction of CO_2 concentration in MRC

According to the mass conservation law, for a type of harmful gas in an MRC under ventilation, the balanced equation can be expressed as

$$V\left[C(\tau+\Delta\tau)-C(\tau)\right]=N\nu\Delta\tau-G\Delta\tau\left[C_{\text{out}}(\tau)-C_{\text{in}}(\tau)\right]. \tag{7}$$

As the air supplied to the MRC is fresh air, $C_{\text{in}}(\tau)$ is a constant. It can be assumed that the concentration of harmful gases in an MRC is uniformly distributed, and the concentration of a type of harmful gas at the outflows is equal to that in the indoor air; that is, $C_{\text{out}}(\tau) = C(\tau)$. By solving the differential Eq. (7), the concentration of a harmful gas in the MRC can be expressed as:

$$C(\tau)=\frac{N\nu}{G}+C_{\text{in}}-\left(\frac{N\nu}{G}+C_{\text{in}}-C_0\right)e^{-\frac{G}{V}\tau}. \tag{8}$$

According to Eq. (8), it can be predicted that the harmful gas concentration in the MRC will gradually tend towards a stable value as time increases, as follows:

$$C_{\text{stable}}=\lim_{\tau\to+\infty}C(\tau)=\frac{N\nu}{G}+C_{\text{in}}. \tag{9}$$

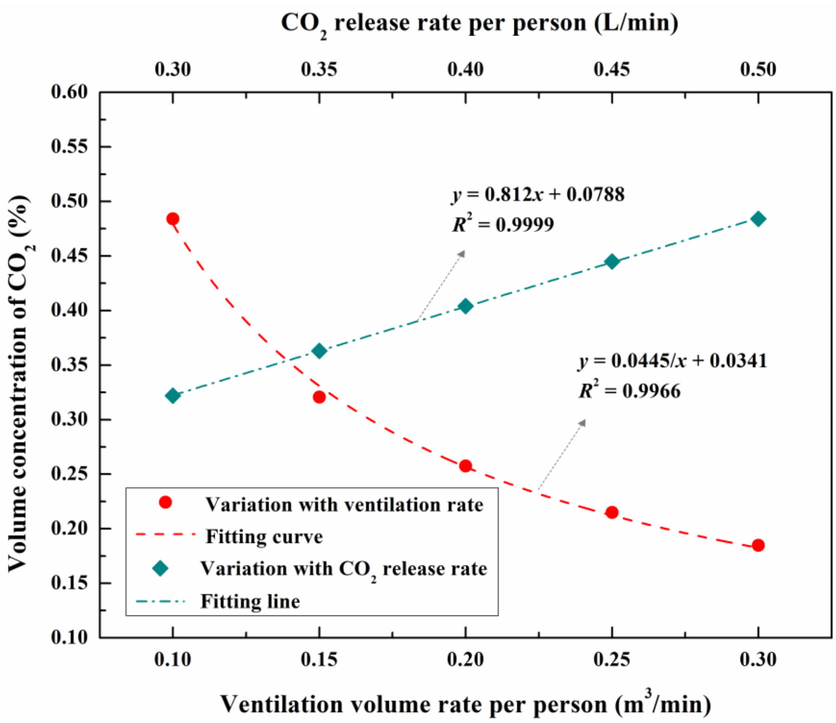

Fig. 16 Variations in CO_2 concentration with ventilation volume rate and CO_2 release rate.

Figure 16 plots the stable average CO_2 concentration varying with the ventilation volume rate and CO_2 release rate, according to the above numerical results. It can be observed that the stable average CO_2 concentration in the MRC decreased monotonically with the increase in the ventilation volume rate when the CO_2 release rate was 0.5 L/min per person; it was inversely proportional to the ventilation volume rate. The fitting formula was $y = 0.0445/x + 0.0341$ with $R^2 = 0.9996$. Moreover, it can easily be found that the stable average CO_2 concentration in the MRC increased linearly with the increase in the CO_2 release rate when the ventilation volume rate was 0.1 m^3/min per person. The fitting formula was $y = 0.812x + 0.0788$ with $R^2 = 0.9999$.

According to the numerical results, the relationship between the CO_2 concentration in an MRC and the ventilation volume rate as well as the CO_2 release rate is the same as that in Eq. (9). The ventilation volume rate and CO_2 release rate are two relatively independent variables. Therefore, the expression of the stable CO_2 concentration in the MRC can be assumed as

$$C_{\text{stable}} = a\frac{Nv}{G} + C_{\text{in}} \,. \tag{10}$$

By introducing the ventilation volume rates and CO_2 release rates, as well as the corresponding stable CO_2 concentration values, in the above analyses into Eq. (10), the optimal solution for *a* can be obtained as 0.92. Thus, the stable CO_2 concentration in the MRC can be calculated as

$$C_{\text{stable}} = 0.92\frac{Nv}{G} + C_{\text{in}} \,. \tag{11}$$

By comparing Eqs. (11) and (9), it can be concluded that, by optimising the ventilation system in the MRC, the stable CO_2 concentration will be lower than the theoretical value, which indicates that improving the ventilation system in an MRC is of significant value for controlling the air quality.

4.4.2 Variations in CO_2 concentration in practical MRC

The average CO_2 release rate has been measured as approximately 0.34 L/min per person when people sit in the MRC, according to an experiment of 50 men residing in an MRC for over 8 h (Zhang, 2013). To simulate the variations in the CO_2 concentration in the MRC in a practical refuge process, a typical case study was considered, in which the CO_2 release rate was 0.34 L/min, the initial CO_2 concentration was 0.03%, and the ventilation volume rate was 0.1 m^3/min per person.

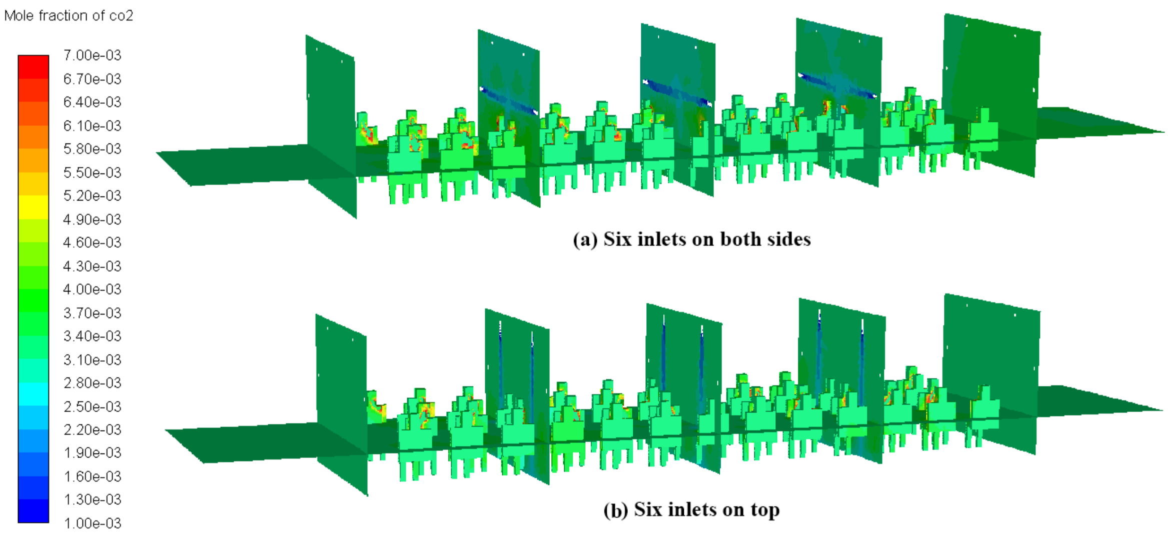

Fig. 17 Distribution of CO_2 concentration in MRC under two different ventilation modes.

Figure 17 illustrates the distribution of the CO_2 concentration under two different ventilation modes: six inlets located on both sides and the top, and one outflow located on each end. It can be observed from Fig. 17 that, in the affected zone of the air inlet jet, the CO_2 concentration was relatively low, at less than 0.3%. Outside the affected zone, the CO_2 concentration distribution was generally uniform, ranging from 0.3% to 0.45%. The CO_2 concentration distribution obtained in these two ventilation modes was fairly uniform.

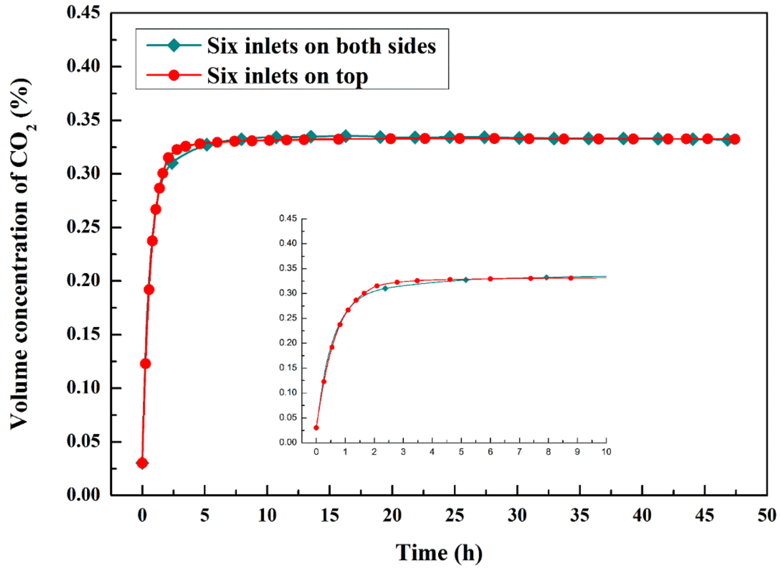

Fig. 18 Variations in average CO_2 concentration in MRC under two different ventilation modes.

Figure 18 plots the variations in the CO_2 concentration with time under two different ventilation modes. It can be observed from Fig. 18 that, when the initial CO_2 concentration was 0.03% and the ventilation rate was 0.1 m^3/min per person, the average CO_2 concentration in the MRC increased rapidly within 2 h, and then tended towards a relatively stable value of 0.33%. In combination with the CO_2 concentration distribution in Fig. 17, it can be concluded that a ventilation volume rate of 0.1 m^3/min per person can control the average CO_2 concentration below 0.35% in a practical MRC, and the CO_2 concentration in the entire room will be less than 0.5%. Meanwhile, Figure 18 indicates that the average CO_2 concentration in the ventilation mode of air supply from the both sides during the initial stage was slightly lower than that in the ventilation mode of air supply from the top. However, the difference was not significant, and the value of the CO_2 concentration difference was less than 0.01%. After reaching the stable state, the average CO_2 concentration in the MRC under the two modes was almost the same.

4.4.3 General ventilation design for common MRC

According to the above analysis, although people's safety may not be threatened when they are exposed to an environment with a CO_2 concentration of 1% or more, their cognitive ability may be affected, which in turn affects their judging abilities in a disaster area. Therefore, it is recommended that the CO_2 concentration of an MRC be limited to 0.5%. The layout of the air inlets and outflows in the MRC plays an important role in controlling the air quality. The air inlets should be arranged in the PCA of the MRC and evenly located on both sides or at the top. The outflows should be located at both ends of the MRC. When placing the inlets at the top, it is preferable to place the outlets at the upper parts of both side walls.

The CO_2 concentration in an MRC can be controlled below 0.5% when the ventilation volume rate reaches 0.1 m^3/min per person, which can meet the oxygen supply and air-purification requirements of the MRC. According to Zhang et al (2018, 2019), for an MRC built in sandstone, when the initial rock temperature is less than 20 °C, the temperature requirement can be met without cooling measures, and when the initial rock temperature reaches 25 °C, the ventilation requirement is 0.1 m^3/min per person. For an MRC with a low temperature in the initial rock, a ventilation volume rate of 0.3 m^3/min per person will increase the air supply difficulty for an MRC and incur unnecessary construction costs. Therefore, it is recommended that the ventilation rate for one person in an MRC is not subjected to a specific restriction, and the ventilation volume rate required for air quality control in an MRC can be calculated by Eq. (11).

5 Conclusions

This work has mainly focused on improving the ventilation system and determining the relationship between the harmful gas concentration and ventilation volume rate in an MRC. An experiment on ventilation to dilute the CO_2 gas in a 50-person MRC was performed. A numerical model was developed and validated against the obtained experimental data. Several control factors, such as the layout of the air inlets and outflows, ventilation volume rate, and CO_2 release rate in the MRC, were investigated in detail. According to the results of the experiment and numerical analyses, the following specific conclusions can be drawn:

(1) The CO_2 concentration in an MRC can be controlled below 0.8% using a ventilation rate of 0.1 m^3/min per person, which can meet the air quality control requirements in the MRC. However, a poor ventilation system may result in excessive concentrations of harmful gases in a local space.

(2) The layout of the air inlets and outflows plays an important role in the distribution of the CO_2 concentration in the MRC. Increasing the number of the air inlets is not necessarily conducive to diluting the CO_2 concentration. For an effective ventilation scheme, it is suggested that six air inlets be located evenly on both sides or at the top of the PCA in the MRC, with one outflow located at each end.

(3) The CO_2 concentration in the MRC decreases inversely with an increase in the ventilation volume rate and increases linearly with an increase in the CO_2 release rate. Under the condition whereby the air inlets and outlets are arranged according to the proposed ventilation system, the value of the average CO_2 concentration in the MRC will be slightly lower than the theoretical result. The average CO_2 concentration can be controlled below 0.5% with a ventilation rate of 0.1 m^3/min and less than 0.2% with a ventilation rate of 0.3 m^3/min per person.

(4) For a practical refuge process, when the ventilation system is arranged according to the proposed mode and the ventilation volume rate is 0.1 m^3/min per person, the CO_2 concentration can reach the RSS within 2 h, the average CO_2 concentration in the MRC is approximately 0.35%, and the CO_2 concentration will be within 0.5% overall.

Acknowledgments

The authors would like to thank the financial support from the National Natural Science Foundation of China (NO. 51678488 and No. 51978575), and the Excellent Doctoral Thesis Cultivation Project of Southwest Jiaotong University (No. D-YB201703) for the financial support for this study.

References

Bacharoudis, E., Vrachopoulos, M.G., Koukou, M.K., Margaris, D., Filios, A.E., Mavrommatis, S.A., 2007. Study of the natural convection phenomena inside a wall solar chimney with one wall adiabatic and one wall under a heat flux. Applied Thermal Engineering. 27, 2266-2275. https://doi.org/10.1016/j.applthermaleng.2007.01.021

Bauer, E.R., Kohler, J.L., 2009. Update on refuge alternatives: research, recommendations and underground deployment. Mining engineering. 61, 51-57. https://www.cdc.gov/niosh/mining/UserFiles/works/pdfs/uorarr.pdf

Boulet, M., Marcos, B., Dostie, M., Moresoli, C., 2010. CFD modeling of heat transfer and flow field in a bakery pilot oven. Journal of food engineering. 97, 393-402. https://doi.org/10.1016/j.jfoodeng.2009.10.034

Charles, D.L., Inoka, E.P., 2012. Evaluation of criteria for the detection of fires in underground conveyor belt haulage ways. Fire Safety Journal. 51, 110-119. https://www.ncbi.nlm.nih.gov/pmc/articles/PMC4641047/

Cheung, T., Schiavon, S., Gall, E.T., Jin, M., Nazaroff, W.W., 2017. Longitudinal assessment of thermal and perceived air quality acceptability in relation to temperature, humidity, and CO_2 exposure in Singapore. Building and Environment. 115, 80-90. https://doi.org/10.1016/j.buildenv.2017.01.014

Du, Y., Wang, S., Jin, L.Z., Wang, S., Gai, W.M., 2018. Experimental investigation and theoretical analysis of the human comfort prediction model in a confined living space. Applied Thermal Engineering. 141, 61-69. https://doi.org/10.1016/j.applthermaleng.2018.05.057

Du, Y., Gai, W.M., Jin, L.Z., 2018. A novel and green CO_2 adsorbent developed with high adsorption properties in a coal mine refuge chamber. Journal of Cleaner Production. 126, 216-229. https://doi.org/10.1016/j.jclepro.2017.12.019

Du, Y., Gai, W.M., Jin, L.Z., Sheng, W., 2017. Thermal comfort model analysis and optimization performance evaluation of a multifunctional ice storage air conditioning system in a confined mine refuge chamber. Energy. 141, 964-974. https://doi.org/10.1016/j.energy.2017.09.123

Gai, W.M., Deng, Y.F., Du, Y., 2016. Adsorption properties of modified soda lime for carbon dioxide removal within the closed environment of a coal mine refuge chamber. Industrial & Engineering Chemistry Research. 40, 10794-10802. https://doi.org/10.1021/acs.iecr.6b02314

Gall, E.T., Cheung, T., Luhung, I., Schiavon, S., Nazaroff, W.W., 2016. Real-time monitoring of personal exposures to carbon dioxide. Building and Environment. 104, 59-67. https://doi.org/10.1016/j.buildenv.2016.04.021

Gao, N., Jin, L.Z., Hu, H.H., Huang, X., Zhou, L., Fan, L.Y., 2015. Potassium superoxide oxygen generation rate and carbon dioxide absorption rate in coal mine refuge chambers. International Journal of Mining Science and Technology. 25, 151-155. https://doi.org/10.1016/j.ijmst.2014.12.001

Gao, N., Jin, L.Z., Wang, L., You, F., 2012. Research and application of oxygen supply system in Changcun coal mine refuge haven. Journal of China Coal Society. 37, 1021-1025. (In Chinese)

Hansen, R., Ingason, H., 2013. Heat release rate measurements of burning mining vehicles in an underground mine. Fire Safety Journal. 61, 12-25. https://doi.org/10.1016/j.firesaf.2013.08.009

He, T.M., 2015. Experimental study on purification by pressure ventilation of coal mine refuge chamber. Industry and Mine Automation. 8, 68-71. (In Chinese)

He, Z., Wu, Q., Wen, L.J., Fu, G., 2019. A process mining approach to improve emergency rescue processes of fatal gas explosion accidents in Chinese coal mines. Safety Science. 111, 154-166. https://doi.org/10.1016/j.ssci.2018.07.006

Jia, S.S., Lai, D.Y., Kang, J., Li, J.Y., Liu, J.J., 2018. Evaluation of relative weights for temperature, CO2, and noise in the aircraft cabin environment. Building and Environment. 131, 108-116. https://doi.org/10.1016/j.buildenv.2018.01.009

Jia, Y.X., Liu, Y.S., Liu, W.H., Li, Z.Y., 2014. Study on purification characteristic of CO_2 and CO within closed environment of coal mine refuge chamber. Separation and Purification Technology.

130, 65-73. https://doi.org/10.1016/j.seppur.2014.04.014
Jin, L.Z., 2013. Research and experiment on air pressure volume of refuge chamber. Proceedings of the 2013 annual conference of the China Occupational Safety and Health Association, Fujian 946-952. (In Chinese)
Kajtár, L., Herczeg, L., 2012. Influence of carbon-dioxide concentration on human well-being and intensity of mental work. Idojaras (Budapest, 1905). 116, 145-169. https://www.researchgate.net/publication/231558578_Influence_of_carbon-dioxide_concentration_on_human_well-being_and_intensity_of_mental_work/link/0912f506c5e44909eb000000/download
Li, Y., Yuan, Y.P., Lia, C.F., Han, X., Zhang X.S., 2018. Human responses to high air temperature, relative humidity and carbon dioxide concentration in underground refuge chamber. Building and Environment. 131, 53-62. https://doi.org/10.1016/j.buildenv.2017.12.038
Liu, W.W., Zhong, W.D., Wargocki, P., 2017. Performance, acute health symptoms and physiological responses during exposure to high air temperature and carbon dioxide concentration. Building and Environment. 114, 96-105. https://doi.org/10.1016/j.buildenv.2016.12.020
Margolis, K.A., Westerman, C.Y.K., Kowalski-Trakofler, K.M., 2011. Underground mine Refuge Chamber Expectations Training: Program development and evaluation. Safety Science. 49, 522-530. https://doi.org/10.1016/j.ssci.2010.12.008
Mejías, C., Jiménez, D., Munoz, A., Reyes-Bozo, L., 2014. Clinical response of 20 people in a mining refuge: study and analysis of functional parameters. Safety Science. 63, 204-210. https://doi.org/10.1016/j.ssci.2013.11.011
National Coal Mine Safety Administration, 2011. Temporary provisions on the construction and management of the coal mine underground emergency refuge system. (In Chinese) http://www.chinacoal-safety.gov.cn/gk/tzgg/201101/t20110127_201854.shtml
National Research Council, 2013. Improving Self-escape From Under-ground Coal Mines. Washington, DC: The National Academies Press. https://doi.org/10.17226/18300.
Persily, A., 2015. Challenges in developing ventilation and indoor air quality standards: The story of ASHRAE Standard 62. Building and Environment. 91, 61-69. https://doi.org/10.1016/j.buildenv.2015.02.026
Piña-Ortiz, A., Hinojosa, J.F., Maytorena, V.M., 2014. Test of turbulence models for natural convection in an open cubic tilted cavity. International Communications in Heat and Mass Transfer. 57, 264-273. https://doi.org/10.1016/j.icheatmasstransfer.2014.08.011
Shao, H., Jiang, S.G., Tao, W.Y., Wu, Z.Y., Zhang, W.Q, Wang, K., 2016. Theoretical and numerical simulation of critical gas supply of refuge chamber. International journal of mining science and technology. 26, 389-393. https://doi.org/10.1016/j.ijmst.2016.02.004
Sørensen, D.N., Nielsen, P.V., 2003. Quality control of computational fluid dynamics in indoor environments. Indoor Air. 13, 2-17. https://doi.org/10.1111/j.1600-0668.2003.00170.x
Trackemas, J.D., Thimons, E.D., Bauer, E.R., Sapko, M.J., Zipf, R. K., et al., 2015. Facilitating the Use of Built-in-place Refuge Alternatives in Mines. DHHS(NIOSH) Publication No. 2015-114, RI 9698, Pittsburgh, PA. https://permanent.access.gpo.gov/gpo58847/2015-114.pdf
Tripathy, D.P., Ala, C.K., 2018. Identification of safety hazards in Indian underground coal mines. Journal of Sustainable Mining. 17, 175-183. https://doi.org/10.1016/j.jsm.2018.07.005
Vaught, C., Brnich, M.J., Mallett, L.G., 2000. Behavioral and Organizational Dimensions of Underground Mine Fires. U.S. Department of Health and Human Services, Pittsburgh, PA. https://www.cdc.gov/niosh/mining/UserFiles/works/pdfs/ic9450.pdf

Wang, L., Cheng, Y.P., Liu, H.Y., 2014. An analysis of fatal gas accidents in Chinese coal mines. Safety Science. 62, 107-113. https://doi.org/10.1016/j.ssci.2013.08.010

Wang, L.J., Wang, Y.L., Cao, Q.Y., Li, X.D., Li, J.Q., et al., 2014. A framework for human error risk analysis of coal mine emergency evacuation in China. Journal of Loss Prevention in the Process Industries. 30, 113-123. https://doi.org/10.1016/j.jlp.2014.05.007

Wang, S., Jin, L.Z., Ou, S.N., Li, Y.G., 2017. Experimental air curtain solution for refuge alternatives in underground mines. Tunnelling and Underground Space Technology. 68, 74-81. https://doi.org/10.1016/j.tust.2017.05.024

Wu, T., Lei. C.W., 2015. On numerical modelling of conjugate turbulent natural convection and radiation in a differentially heated cavity. International Journal of Heat and Mass Transfer. 91, 454-466. https://doi.org/10.1016/j.ijheatmasstransfer.2015.07.113

You, F., Jin, L.Z., Han, H.R., Gao, N., 2012. Research on air supply to refuge chamber. China Safety Science Journal. 22, 116-120. (In Chinese)

Zhai, Y.C., Li, M.H., Gao, S.R., Yang, L., Zhang, H., Arens, E., Gao, Y.F., 2018. Indirect calorimetry on the metabolic rate of sitting, standing and walking office activities. Building and Environment. 145, 77-84. https://doi.org/10.1016/j.buildenv.2018.09.011

Zhang, S.Z., Wu, Z.Z., Zhang, R., Kang, J.N., 2012. Dynamic numerical simulation of coal mine fire for escape capsule installation. Safety Science. 50, 600-606. https://doi.org/10.1016/j.ssci.2011.09.007

Zhang, X.J., Wargocki, P., Lian, Z.W., 2016. Human responses to carbon dioxide, a follow-up study at recommended exposure limits in non-industrial environments. Building and environment 100, 162-171. https://doi.org/10.1016/j.buildenv.2016.02.014

Zhang, Z.J., 2013. Theoretical study on cooling technology of a coal mine refuge chamber. Master Degree Dissertation of Chongqing Research Institute of Coal Research Institute. (In Chinese)

Zhang, Z.J., Yuan, Y.P., Wang, K.Q., Gao, X.K., Cao, X.L., 2016. Experimental investigation on influencing factors of air curtain systems barrier efficiency for mine refuge chamber. Process Safety and Environmental Protection. 102, 534-546. https://doi.org/10.1016/j.psep.2016.05.008

Zhang, Z.J., Yuan, Y.P., Wang, K.Q., 2017. Effects of number and layout of air purification devices in mine refuge chamber. Process Safety and Environmental Protection. 105, 338-347. https://doi.org/10.1016/j.psep.2016.11.023

Zhang, Z.J., Day, R., Wang, K.Q., Wu, H.W., Yuan, Y.P., 2018. Thermal performance analysis of an underground closed chamber with human body heat sources under natural convection. Applied Thermal Engineering. 145, 453-463. https://doi.org/10.1016/j.applthermaleng.2018.09.068

Zhang, Z.J., Wu, H.W., Wang, K.Q., Day, R., Yuan, Y.P., 2019. Thermal performance of a mine refuge chamber with human body heat sources under ventilation, Applied Thermal Engineering 162, 114243. https://doi.org/10.1016/j.applthermaleng.2019.114243

Zhu, Y.F., Wang, D.M., Shao, Z.L., Xu, C.H., Zhu, X.L., Qia, X.Y., Liu, F.M., 2019. A statistical analysis of coalmine fires and explosions in China. Process Safety and Environmental Protection. 121, 357-366. https://doi.org/10.1016/j.psep.2018.11.013